

*Electronic Supplementary Information  
For*

**Fluorinated *meso*-tetraaryl Pt(II)-porphyrins: Structure, Photophysical,  
Electrochemical and Phosphorescent Oxygen Sensing Studies**

**Chellaiah Arunkumar<sup>a\*</sup>, Fasalu Rahman Kooriyaden<sup>a</sup>, Xiaochen Zhang<sup>b</sup>, Subramaniam Sujatha<sup>a</sup> and Jianzhang Zhao<sup>b</sup>**

<sup>a</sup>Bioinorganic Materials Research Laboratory, Department of Chemistry, National Institute of Technology Calicut, Kozhikode, Kerala, India - 673 601. E-mail: arunkumarc@nitc.ac.in

<sup>b</sup>State Key Laboratory of Fine Chemicals, School of Chemical Engineering, Dalian University of Technology, E 208 Western Campus, 2 Ling-Gong Road, Dalian 116012, P.R. China.

Contents

**Figure S1.** <sup>1</sup>H NMR spectrum of PtTPP, **F1**.

**Figure S2.** <sup>1</sup>H NMR spectrum of PtT(2,3,4,5,6-PFP)P, **F2**.

**Figure S3.** <sup>1</sup>H NMR spectrum of PtT(2,6-DFP)P, **F3**.

**Figure S4.** <sup>1</sup>H NMR spectrum of PtT(3,5-DFP)P, **F4**.

**Figure S5.** <sup>1</sup>H NMR spectrum of PtT(2,4,6-TFP)P, **F5**.

**Figure S6.** <sup>1</sup>H NMR spectrum of PtT(4-TFMP)P, **F7**.

**Figure S7.** <sup>1</sup>H NMR spectrum of PtT(3,5-DTFMP)P, **F8**.

**Figure S8.** Emission spectra of PtTPP, **F1** in solution under N<sub>2</sub>, air and O<sub>2</sub>. ( $\lambda_{\text{ex}} = 402$  nm)

**Figure S9.** Emission spectra of PtTPP, **F2** in solution under N<sub>2</sub>, air and O<sub>2</sub>. ( $\lambda_{\text{ex}} = 392$  nm)

**Figure S10.** Emission spectra of PtTPP, **F3** in solution under N<sub>2</sub>, air and O<sub>2</sub>. ( $\lambda_{\text{ex}} = 395$  nm)

**Figure S11.** Emission spectra of PtTPP, **F4** in solution under N<sub>2</sub>, air and O<sub>2</sub>. ( $\lambda_{\text{ex}} = 399$  nm)

**Figure S12.** Emission spectra of PtTPP, **F5** in solution under N<sub>2</sub>, air and O<sub>2</sub>. ( $\lambda_{\text{ex}} = 393$  nm)

**Figure S13.** Emission spectra of PtTPP, **F6** in solution under N<sub>2</sub>, air and O<sub>2</sub>. ( $\lambda_{\text{ex}} = 402$  nm)

**Figure S14.** Emission spectra of PtTPP, **F7** in solution under N<sub>2</sub>, air and O<sub>2</sub>. ( $\lambda_{\text{ex}} = 401$  nm)

**Figure S15.** Phosphorescent emission change of the complex, **F1** films vs. O<sub>2</sub>/N<sub>2</sub> saturation switch.  $\lambda_{\text{ex}} = 402$  nm,  $\lambda_{\text{em}} = 666$  nm.

**Figure S16.** Phosphorescent emission change of the complex, **F2** films vs. O<sub>2</sub>/N<sub>2</sub> saturation switch.  $\lambda_{\text{ex}} = 392 \text{ nm}$ ,  $\lambda_{\text{em}} = 649 \text{ nm}$ .

**Figure S17.** Phosphorescent emission change of the complex, **F3** films vs. O<sub>2</sub>/N<sub>2</sub> saturation switch.  $\lambda_{\text{ex}} = 400 \text{ nm}$ ,  $\lambda_{\text{em}} = 644 \text{ nm}$ .

**Figure S18.** Phosphorescent emission change of the complex, **F4** films vs. O<sub>2</sub>/N<sub>2</sub> saturation switch.  $\lambda_{\text{ex}} = 395 \text{ nm}$ ,  $\lambda_{\text{em}} = 643 \text{ nm}$ .

**Figure S19.** Phosphorescent emission change of the complex, **F5** films vs. O<sub>2</sub>/N<sub>2</sub> saturation switch.  $\lambda_{\text{ex}} = 393 \text{ nm}$ ,  $\lambda_{\text{em}} = 646 \text{ nm}$ .

**Figure S20.** Phosphorescent emission change of the complex, **F6** films vs. O<sub>2</sub>/N<sub>2</sub> saturation switch.  $\lambda_{\text{ex}} = 402 \text{ nm}$ ,  $\lambda_{\text{em}} = 650 \text{ nm}$ .

**Figure S21.** Phosphorescent emission change of the complex, **F7** films vs. O<sub>2</sub>/N<sub>2</sub> saturation switch.  $\lambda_{\text{ex}} = 401 \text{ nm}$ ,  $\lambda_{\text{em}} = 655 \text{ nm}$ .

**Figure S22.** (a) Dynamic response of **F1** films vs. small steps of variation of O<sub>2</sub> partial pressure.  $\lambda_{\text{ex}} = 402 \text{ nm}$ ,  $\lambda_{\text{em}} = 666 \text{ nm}$ ; (b) Fitting of the oxygen sensing property of the IMPEK-C films of complex, **F1** based on the two site model (eqn(1)).

**Figure S23.** (a) Dynamic response of **F2** films vs. small steps of variation of O<sub>2</sub> partial pressure.  $\lambda_{\text{ex}} = 392 \text{ nm}$ ,  $\lambda_{\text{em}} = 649 \text{ nm}$ ; (b) Fitting of the oxygen sensing property of the IMPEK-C films of complex, **F2** based on the two site model (eqn(1)).

**Figure S24.** (a) Dynamic response of **F3** films vs. small steps of variation of O<sub>2</sub> partial pressure.  $\lambda_{\text{ex}} = 395 \text{ nm}$ ,  $\lambda_{\text{em}} = 643 \text{ nm}$ ; (b) Fitting of the oxygen sensing property of the IMPEK-C films of complex, **F3** based on the two site model (eqn(1)).

**Figure S25.** (a) Dynamic response of **F4** films vs. small steps of variation of O<sub>2</sub> partial pressure.  $\lambda_{\text{ex}} = 399 \text{ nm}$ ,  $\lambda_{\text{em}} = 646 \text{ nm}$ ; (b) Fitting of the oxygen sensing property of the IMPEK-C films of complex, **F4** based on the two site model (eqn(1)).

**Figure S26.** (a) Dynamic response of **F5** films vs. small steps of variation of O<sub>2</sub> partial pressure.  $\lambda_{\text{ex}} = 393 \text{ nm}$ ,  $\lambda_{\text{em}} = 646 \text{ nm}$ ; (b) Fitting of the oxygen sensing property of the IMPEK-C films of complex, **F5** based on the two site model (eqn(1)).

**Figure S27.** (a) Dynamic response of **F6** films vs. small steps of variation of O<sub>2</sub> partial pressure.  $\lambda_{\text{ex}} = 402 \text{ nm}$ ,  $\lambda_{\text{em}} = 650 \text{ nm}$ ; (b) Fitting of the oxygen sensing property of the IMPEK-C films of complex, **F6** based on the two site model (eqn(1)).

**Figure S28.** (a) Dynamic response of **F7** films vs. small steps of variation of O<sub>2</sub> partial pressure.  $\lambda_{\text{ex}} = 401 \text{ nm}$ ,  $\lambda_{\text{em}} = 655 \text{ nm}$ ; (b) Fitting of the oxygen sensing property of the IMPEK-C films of complex, **F7** based on the two site model (eqn(1)).

**Table S1.** Luminescent lifetime for complexes, **F1-F8**.

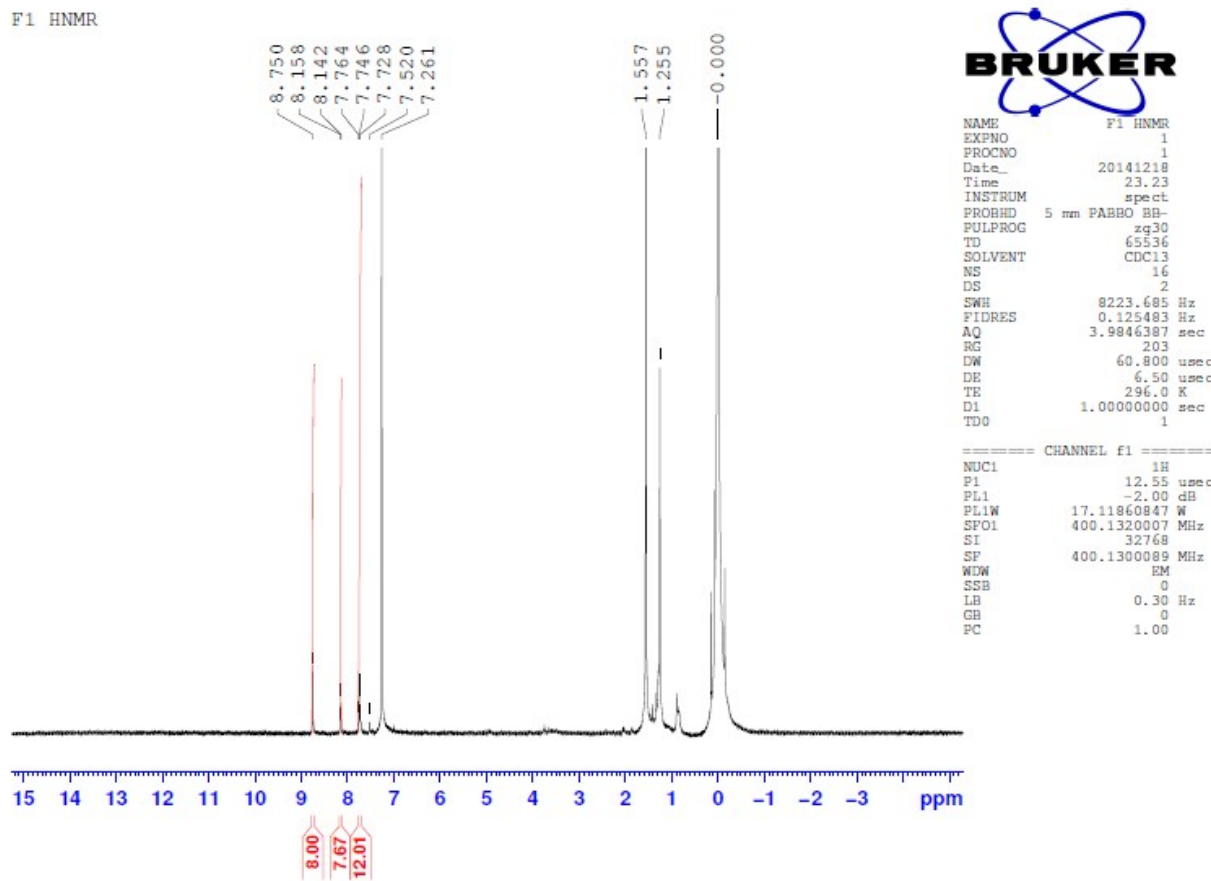


**Figure S1.**  $^1\text{H}$  NMR spectrum of PtTPP, **F1**.

F2 HNMR

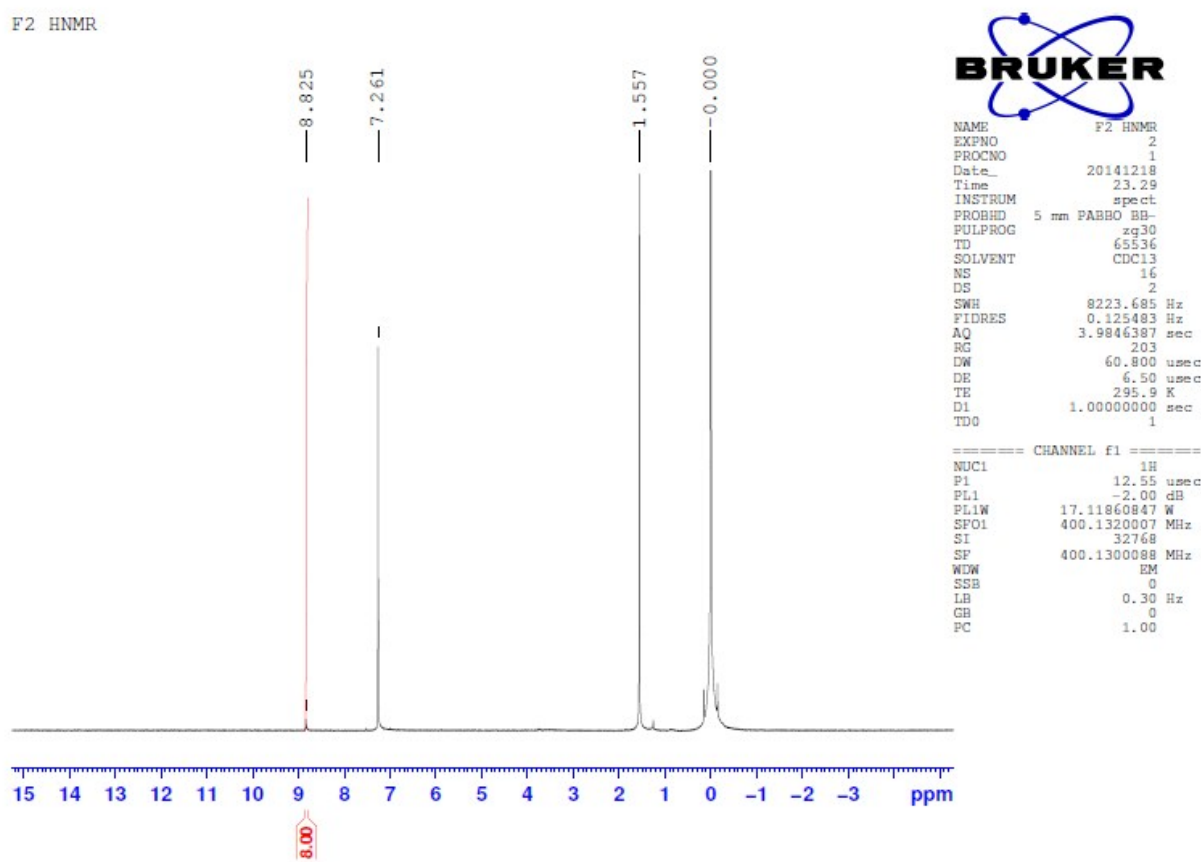


**Figure S2.**  $^1\text{H}$  NMR spectrum of PtT(2,3,4,5,6-PFP)P, F2.

F3 HNMR

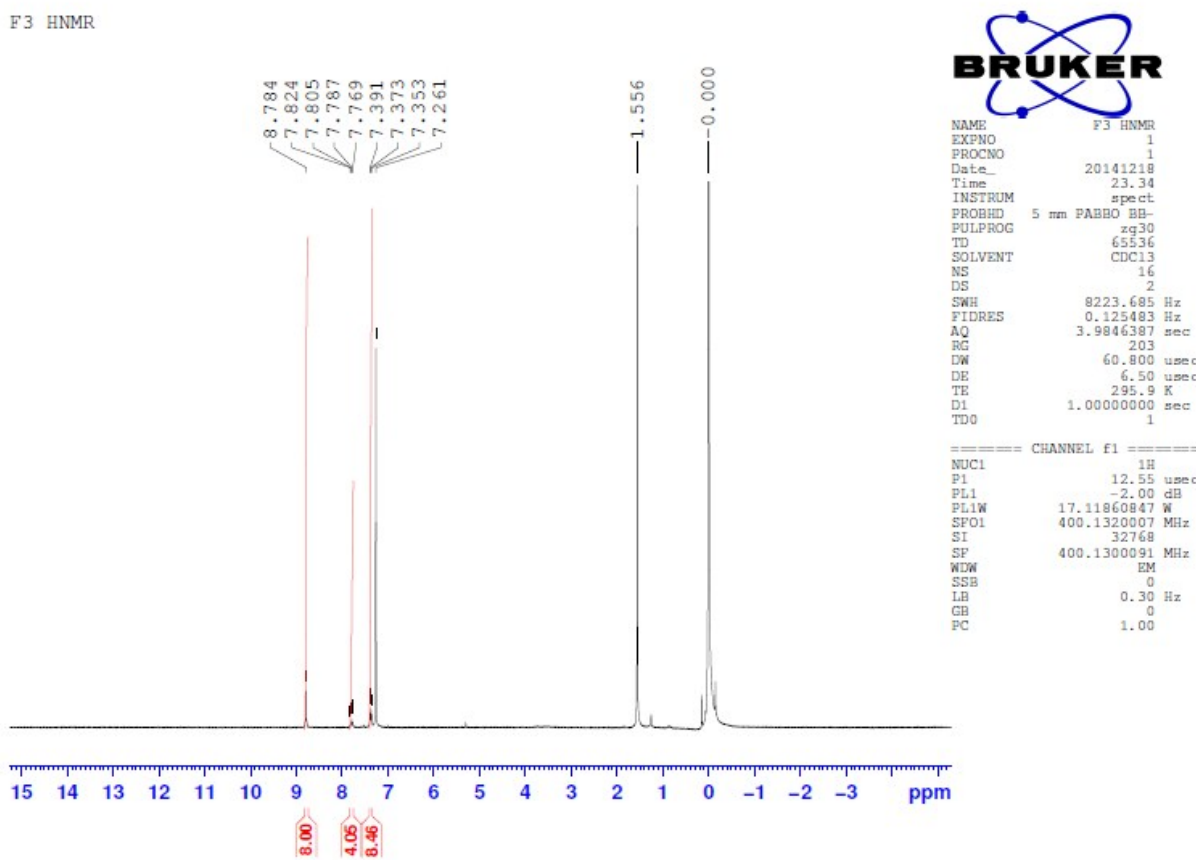


**Figure S3.**  $^1\text{H}$  NMR spectrum of PtT(2,6-DFP)P, **F3**.

F4 HNMR

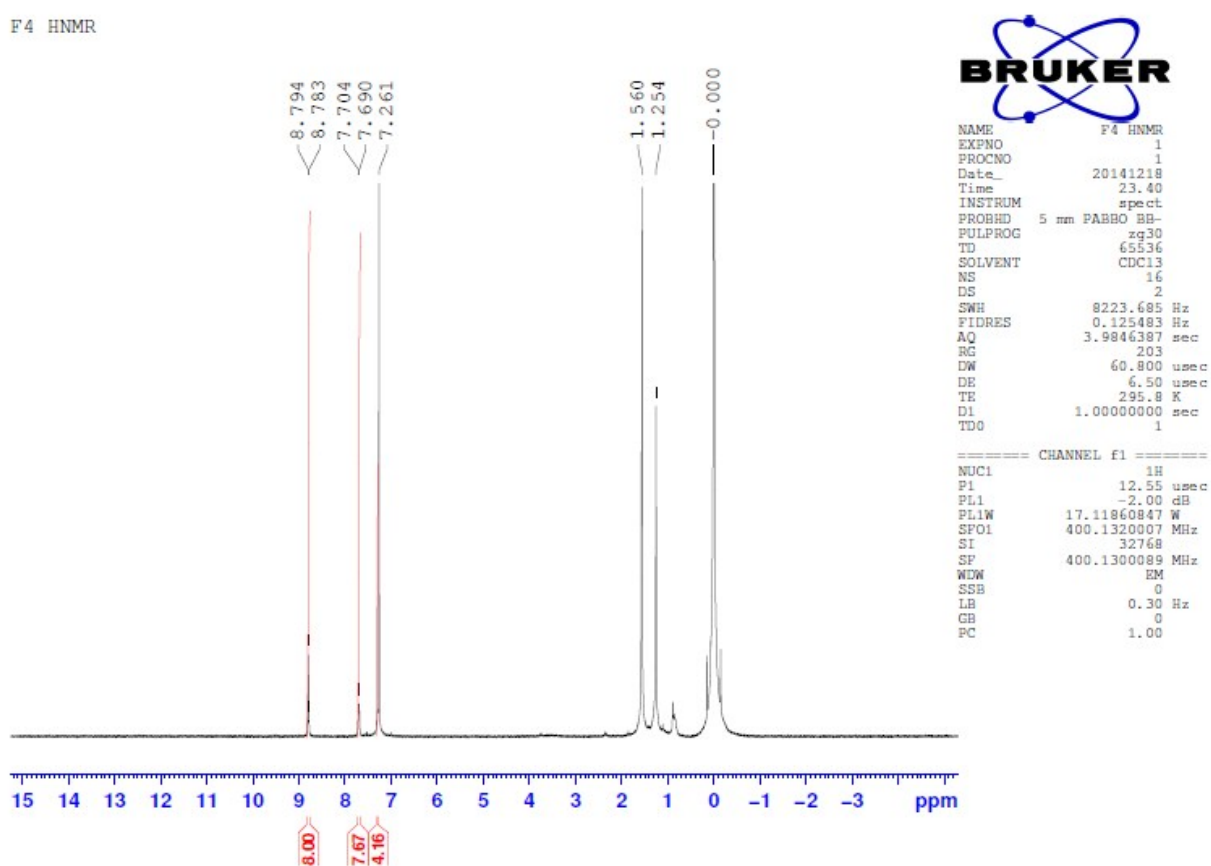


**Figure S4.**  $^1\text{H}$  NMR spectrum of PtT(3,5-DFP)P, F4.

F5 HNMR

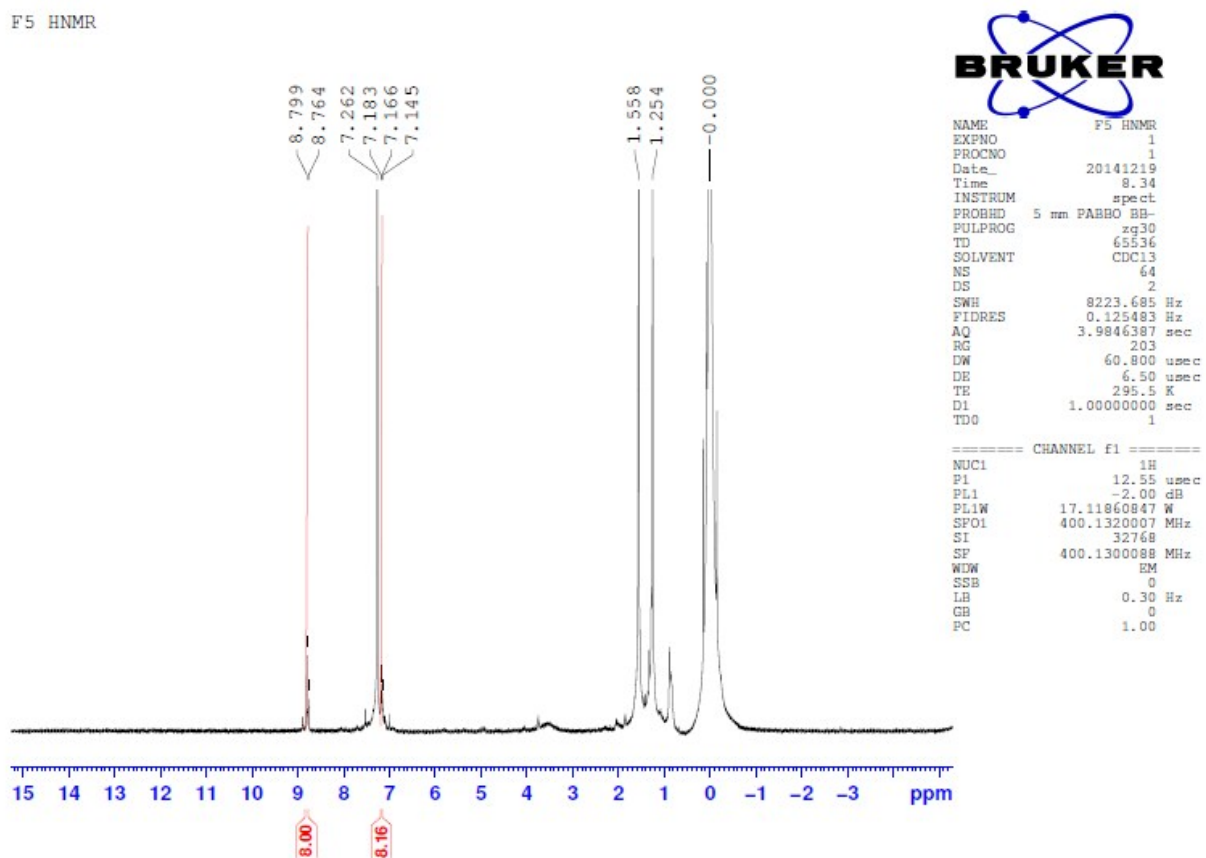


**Figure S5.**  $^1\text{H}$  NMR spectrum of PtT(2,4,6-TFP)P, **F5**.

F6 HNMR

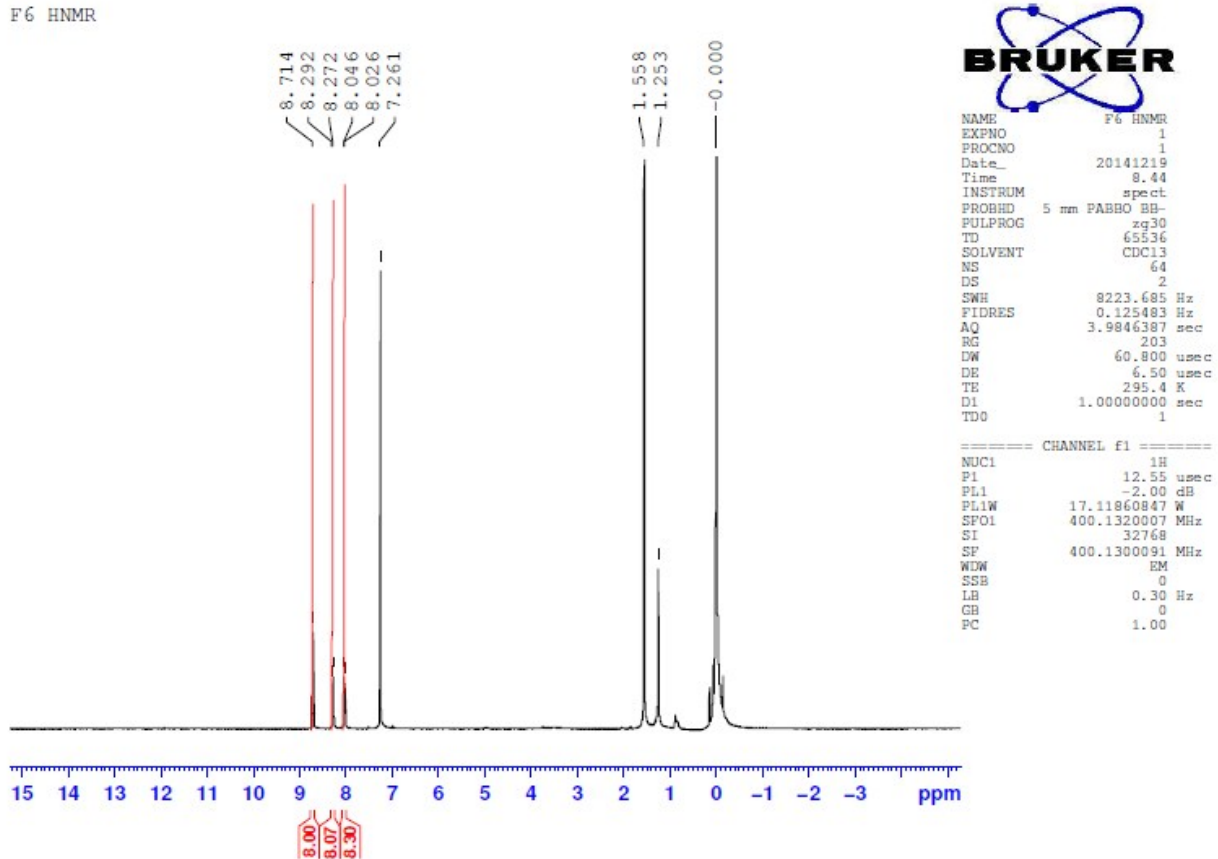


**Figure S6.**  $^1\text{H}$  NMR spectrum of PtT(4-TFMP)P, **F7**.

F7 HNMR

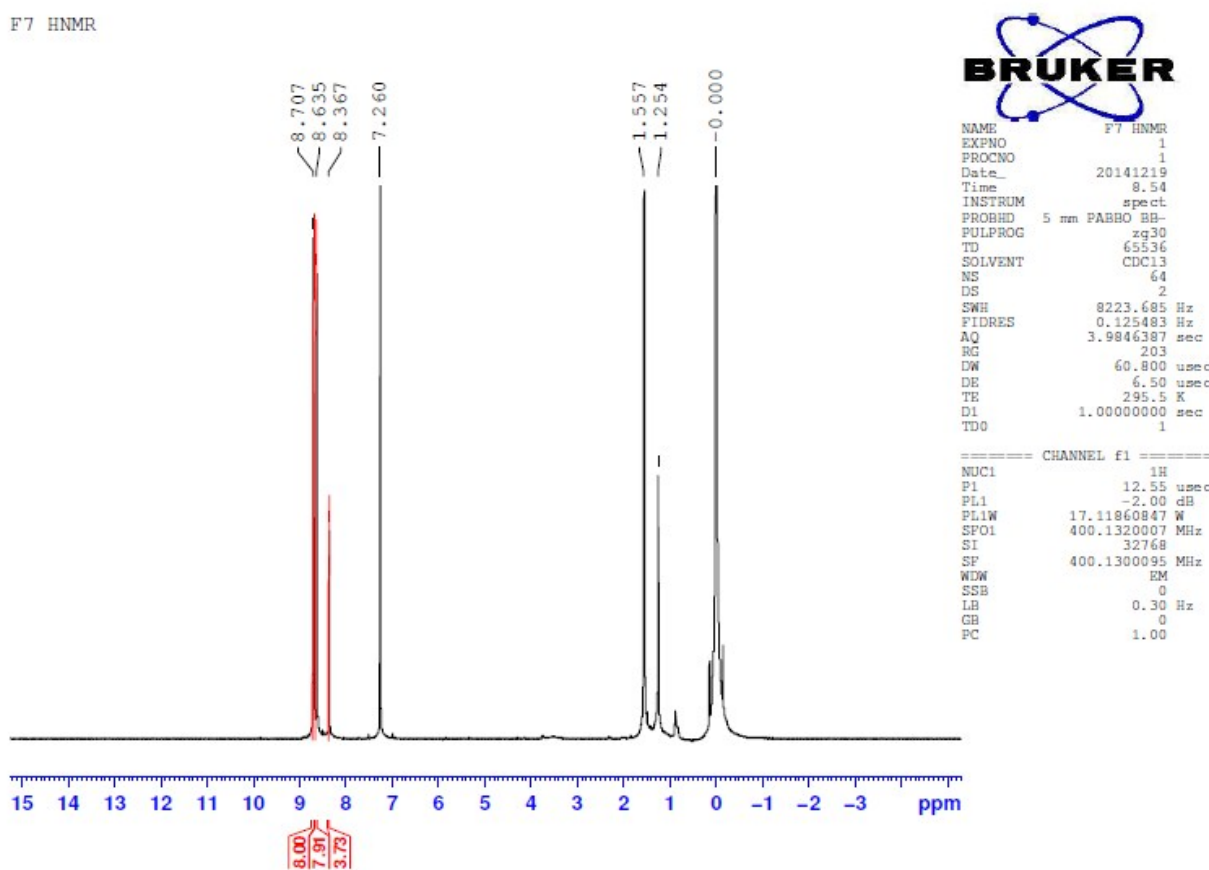


**Figure S7.**  $^1\text{H}$  NMR spectrum of PtT(3,5-DTFMP)P, **F8**.

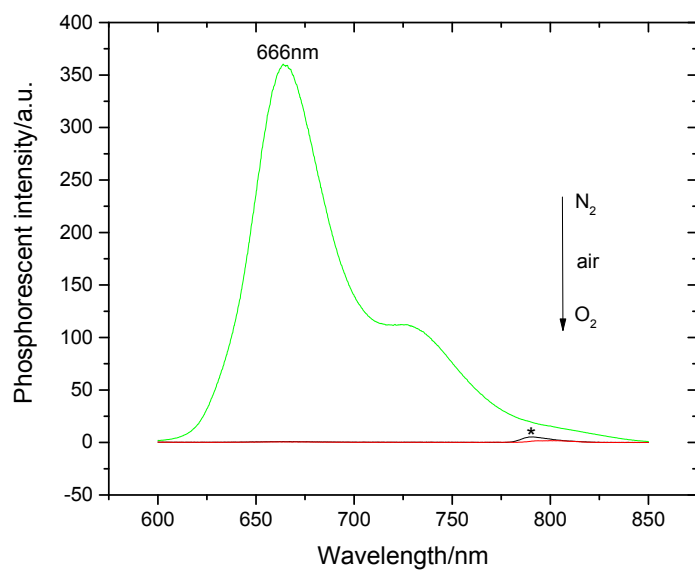


**Figure S8.** Emission spectra of PtTPP, **F1** in solution under  $N_2$ , air and  $O_2$ . ( $\lambda_{\text{ex}} = 402$  nm)

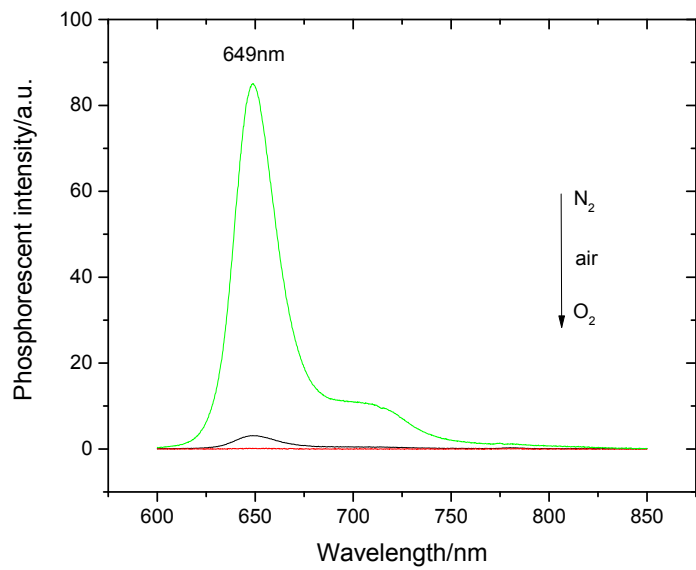


**Figure S9.** Emission spectra of PtTPP, **F2** in solution under  $N_2$ , air and  $O_2$ . ( $\lambda_{\text{ex}} = 392$  nm)

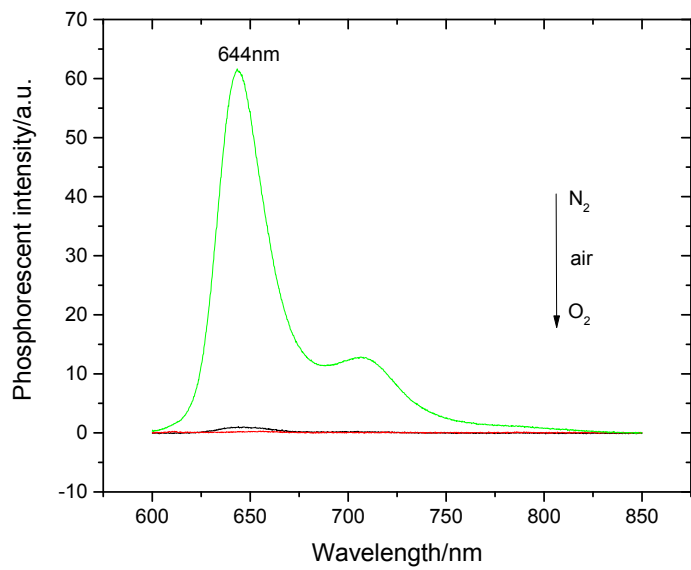


**Figure S10.** Emission spectra of PtTPP, **F3** in solution under  $N_2$ , air and  $O_2$ . ( $\lambda_{\text{ex}} = 395 \text{ nm}$ )

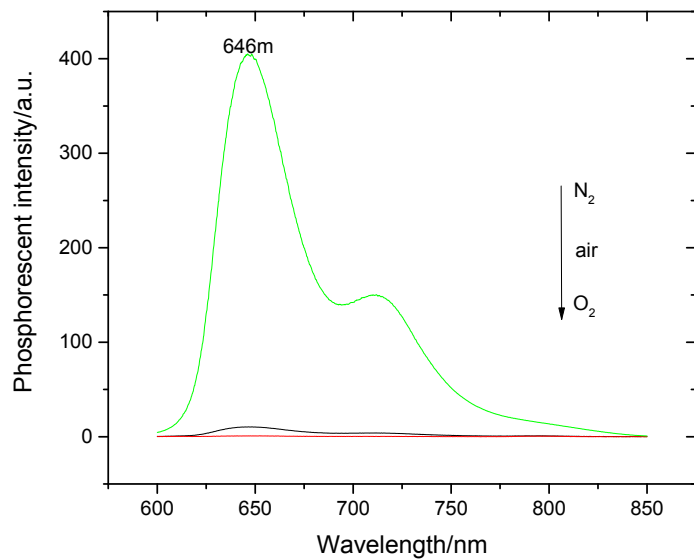


**Figure S11.** Emission spectra of PtTPP, **F4** in solution under  $N_2$ , air and  $O_2$ . ( $\lambda_{\text{ex}} = 399$  nm)

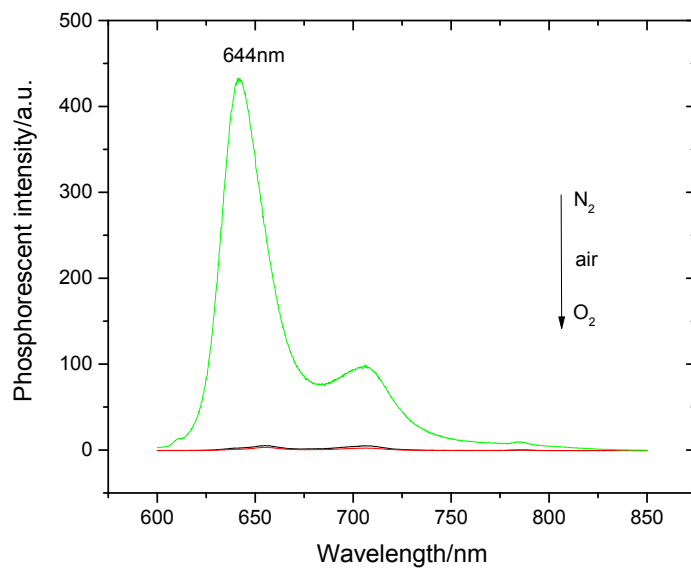


**Figure S12.** Emission spectra of PtTPP, **F5** in solution under N<sub>2</sub>, air and O<sub>2</sub>. ( $\lambda_{\text{ex}} = 393$  nm)

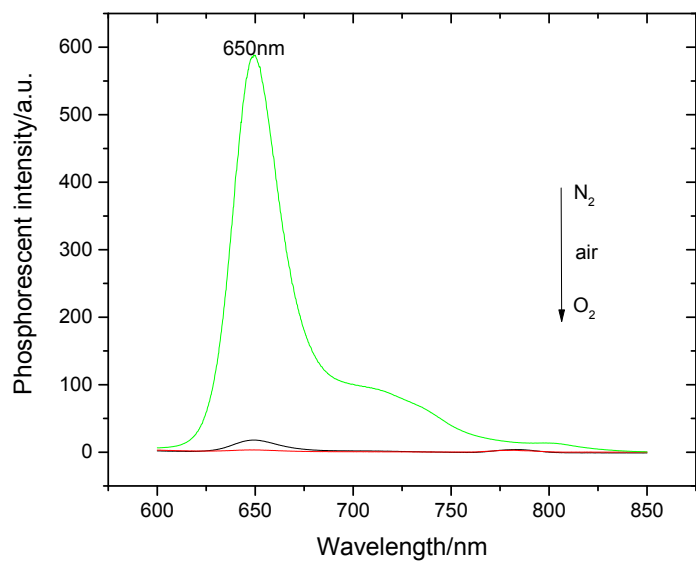


**Figure S13.** Emission spectra of PtTPP, **F6** in solution under  $N_2$ , air and  $O_2$ . ( $\lambda_{\text{ex}} = 402 \text{ nm}$ )

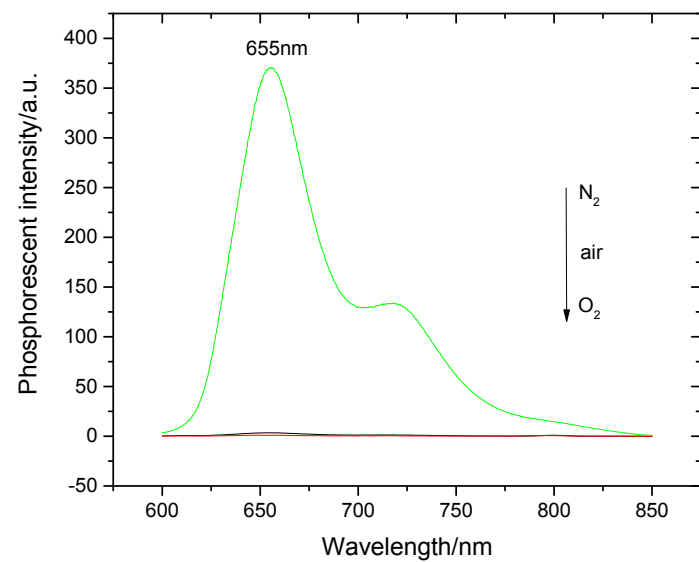


**Figure S14.** Emission spectra of PtTPP, F7 in solution under  $\text{N}_2$ , air and  $\text{O}_2$ . ( $\lambda_{\text{ex}} = 401 \text{ nm}$ )

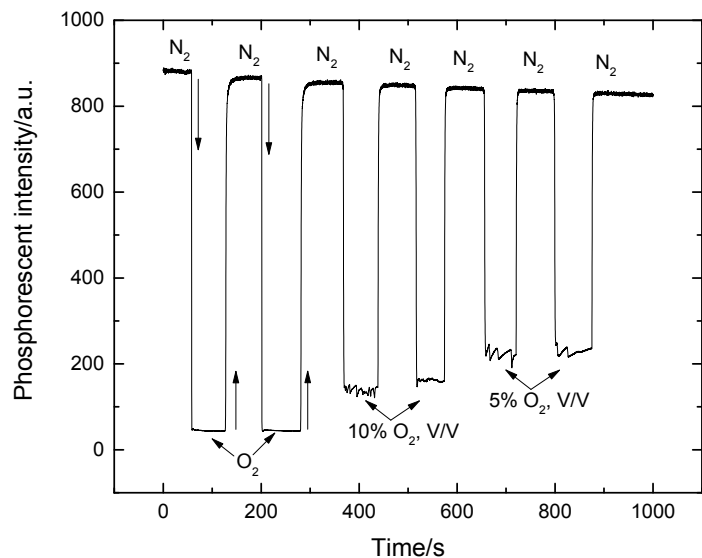


**Figure S15.** Phosphorescent emission change of the complex, **F1** films vs. O<sub>2</sub>/N<sub>2</sub> saturation switch.  $\lambda_{\text{ex}} = 402 \text{ nm}$ ,  $\lambda_{\text{em}} = 666 \text{ nm}$ .

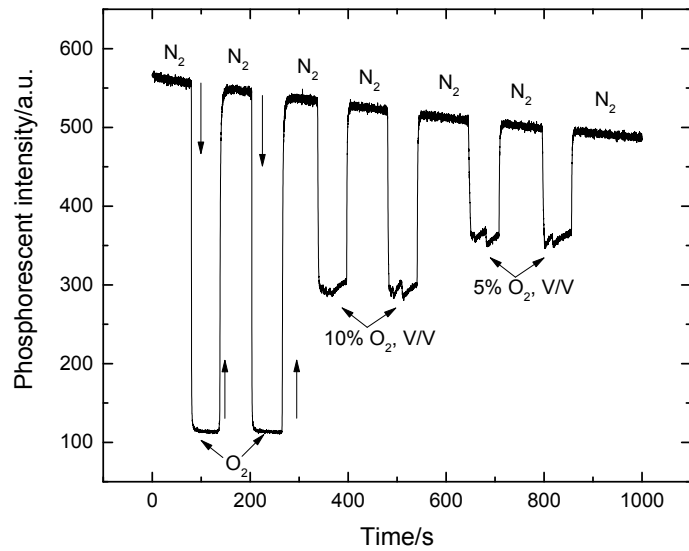


**Figure S16.** Phosphorescent emission change of the complex, **F2** films vs.  $O_2/N_2$  saturation switch.  $\lambda_{\text{ex}} = 392 \text{ nm}$ ,  $\lambda_{\text{em}} = 649 \text{ nm}$ .

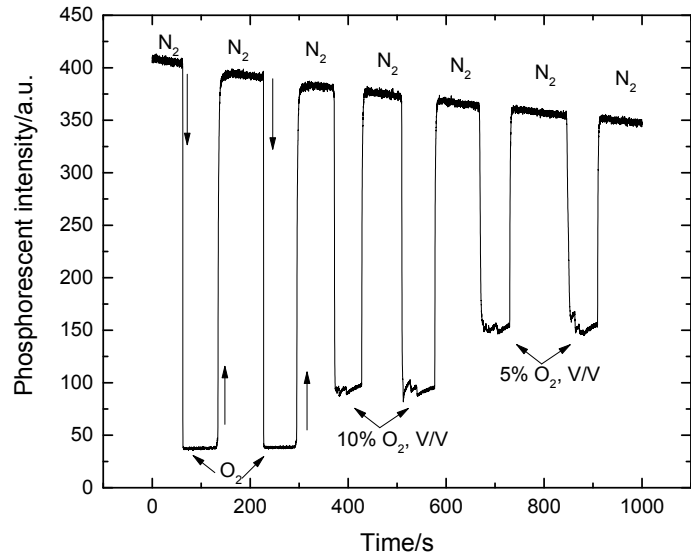


**Figure S17.** Phosphorescent emission change of the complex, **F3** films vs.  $O_2/N_2$  saturation switch.  $\lambda_{\text{ex}} = 400$  nm,  $\lambda_{\text{em}} = 644$  nm.

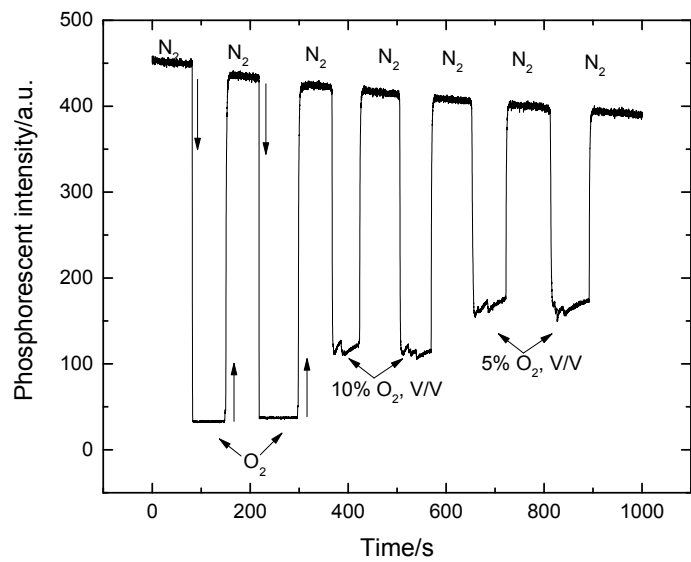


**Figure S18.** Phosphorescent emission change of the complex, **F4** films vs. O<sub>2</sub>/N<sub>2</sub> saturation switch.  $\lambda_{\text{ex}} = 395 \text{ nm}$ ,  $\lambda_{\text{em}} = 643 \text{ nm}$ .

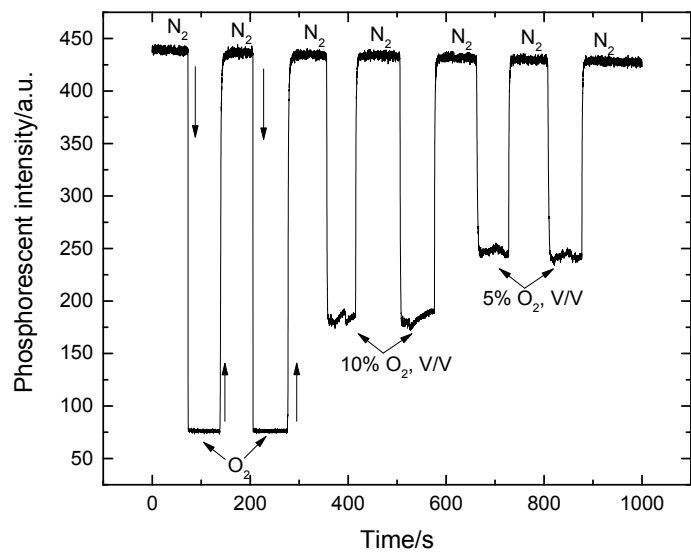


**Figure S19.** Phosphorescent emission change of the complex, **F5** films vs. O<sub>2</sub>/N<sub>2</sub> saturation switch.  $\lambda_{\text{ex}} = 393 \text{ nm}$ ,  $\lambda_{\text{em}} = 646 \text{ nm}$ .

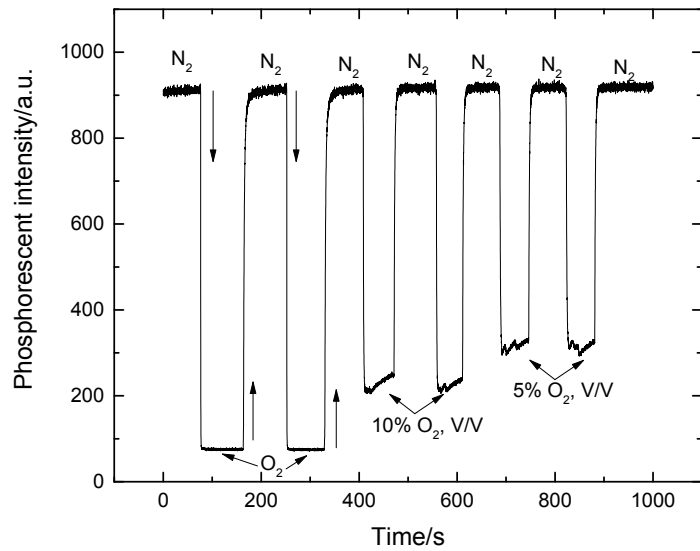


**Figure S20.** Phosphorescent emission change of the complex, **F6** films vs. O<sub>2</sub>/N<sub>2</sub> saturation switch.  $\lambda_{\text{ex}} = 402 \text{ nm}$ ,  $\lambda_{\text{em}} = 650 \text{ nm}$ .

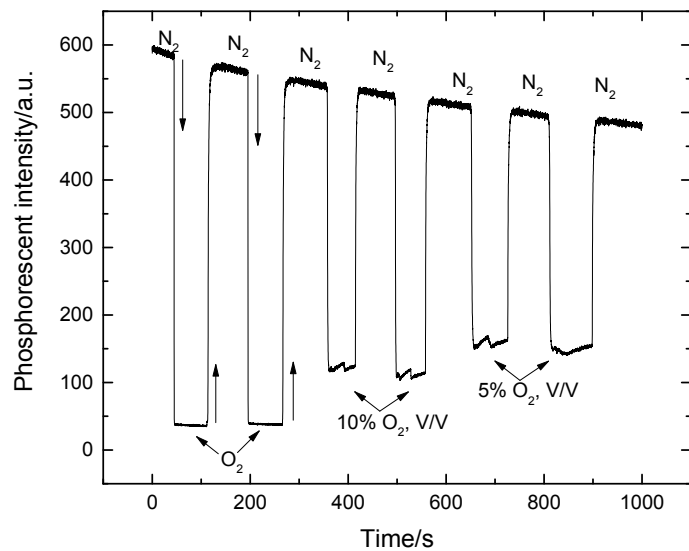


**Figure S21.** Phosphorescent emission change of the complex, F7 films vs. O<sub>2</sub>/N<sub>2</sub> saturation switch.  $\lambda_{\text{ex}} = 401 \text{ nm}$ ,  $\lambda_{\text{em}} = 655 \text{ nm}$ .

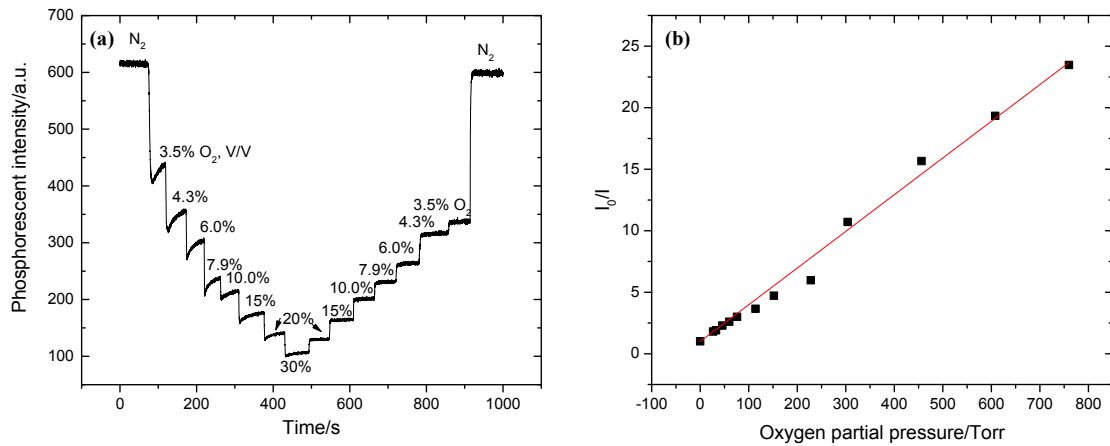


**Figure S22.** (a) Dynamic response of **F1** films vs. small steps of variation of O<sub>2</sub> partial pressure.  $\lambda_{\text{ex}} = 402 \text{ nm}$ ,  $\lambda_{\text{em}} = 666 \text{ nm}$ ; (b) Fitting of the oxygen sensing property of the IMPEK-C films of complex, **F1** based on the two site model (eqn(1)).

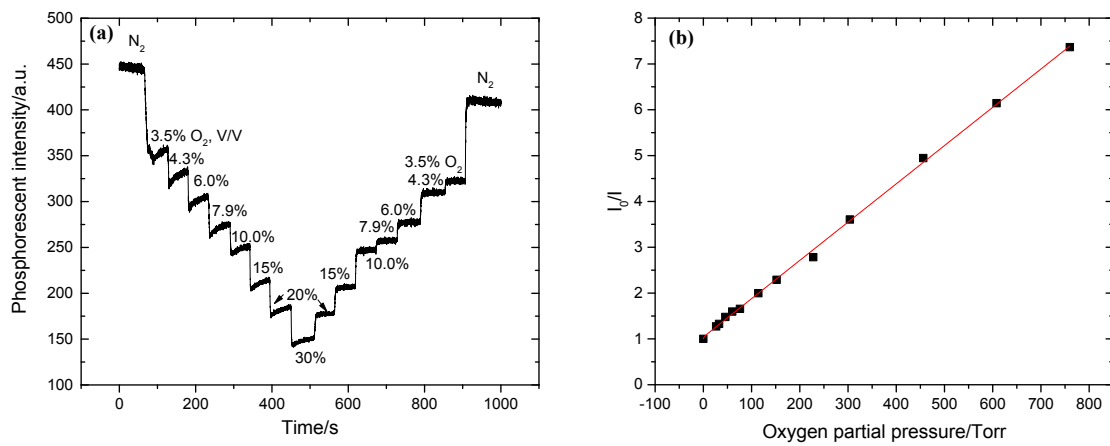


**Figure S23.** (a) Dynamic response of **F2** films vs. small steps of variation of O<sub>2</sub> partial pressure.  $\lambda_{\text{ex}} = 392$  nm,  $\lambda_{\text{em}} = 649$  nm; (b) Fitting of the oxygen sensing property of the IMPEK-C films of complex, **F2** based on the two site model (eqn(1)).

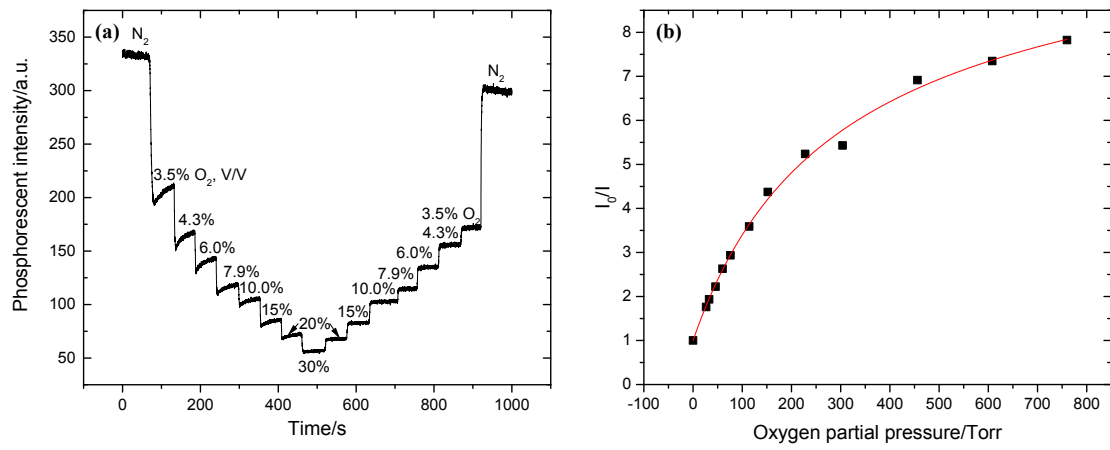


**Figure S24.** (a) Dynamic response of **F3** films vs. small steps of variation of O<sub>2</sub> partial pressure.  $\lambda_{\text{ex}} = 395$  nm,  $\lambda_{\text{em}} = 643$  nm; (b) Fitting of the oxygen sensing property of the IMPEK-C films of complex, **F3** based on the two site model (eqn(1)).

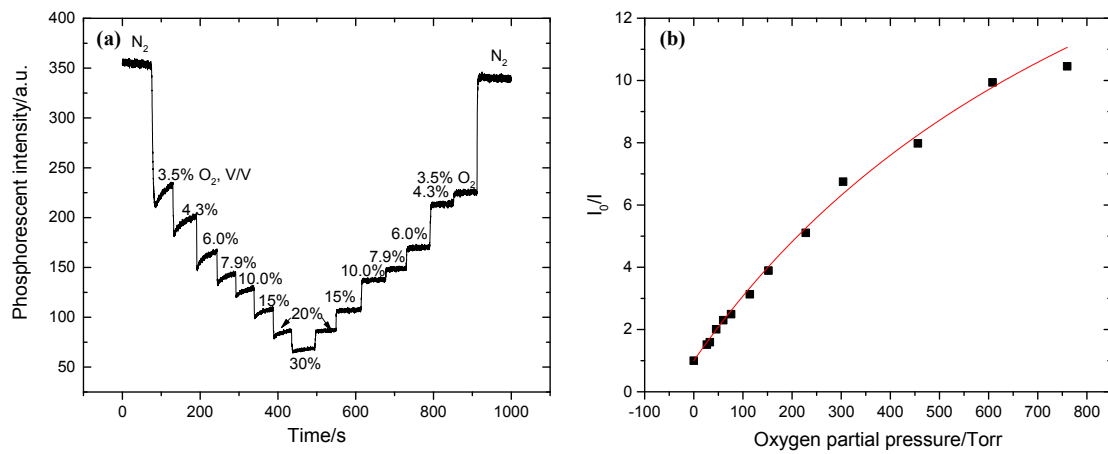


**Figure S25.** (a) Dynamic response of **F4** films vs. small steps of variation of O<sub>2</sub> partial pressure.  $\lambda_{\text{ex}} = 399 \text{ nm}$ ,  $\lambda_{\text{em}} = 646 \text{ nm}$ ; (b) Fitting of the oxygen sensing property of the IMPEK-C films of complex, **F4** based on the two site model (eqn(1)).

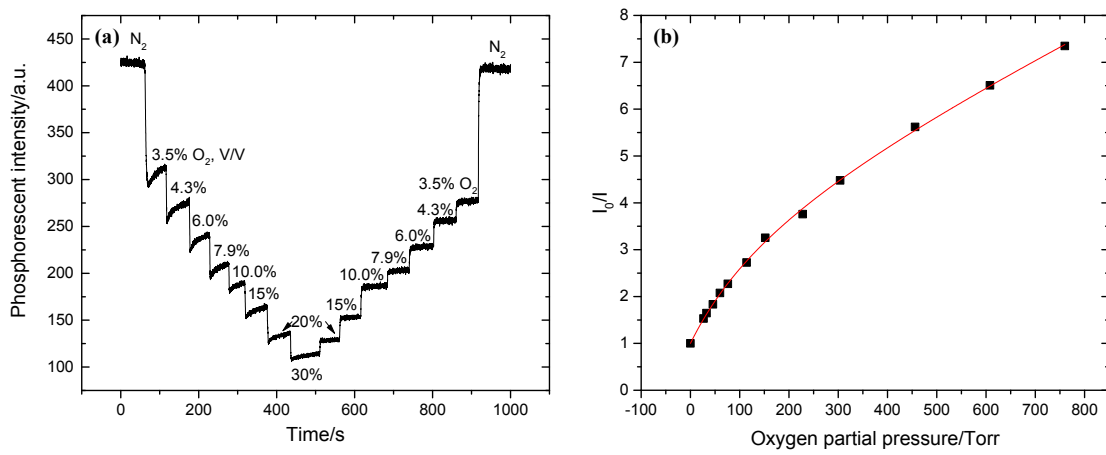


**Figure S26.** (a) Dynamic response of **F5** films vs. small steps of variation of O<sub>2</sub> partial pressure.  $\lambda_{\text{ex}} = 393$  nm,  $\lambda_{\text{em}} = 646$  nm; (b) Fitting of the oxygen sensing property of the IMPEK-C films of complex, **F5** based on the two site model (eqn(1)).

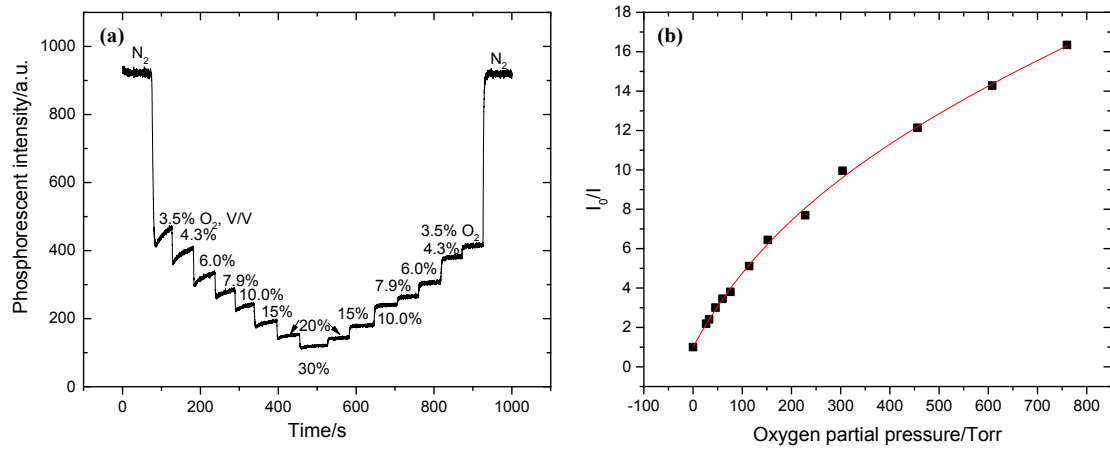


**Figure S27.** (a) Dynamic response of **F6** films vs. small steps of variation of O<sub>2</sub> partial pressure.  $\lambda_{\text{ex}} = 402 \text{ nm}$ ,  $\lambda_{\text{em}} = 650 \text{ nm}$ ; (b) Fitting of the oxygen sensing property of the IMPEK-C films of complex, **F6** based on the two site model (eqn(1)).

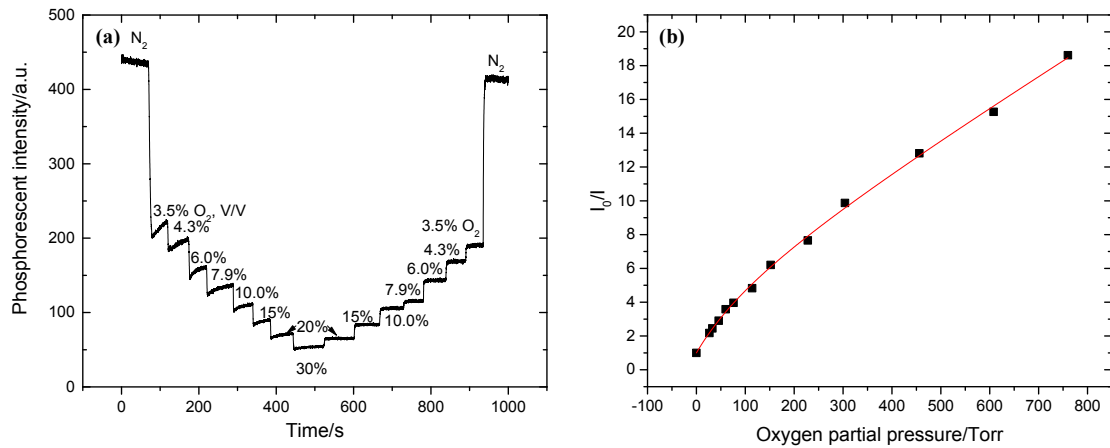


**Figure S28.** (a) Dynamic response of F7 films vs. small steps of variation of O<sub>2</sub> partial pressure.  $\lambda_{\text{ex}} = 401 \text{ nm}$ ,  $\lambda_{\text{em}} = 655 \text{ nm}$ ; (b) Fitting of the oxygen sensing property of the IMPEK-C films of complex, F7 based on the two site model (eqn(1)).

**Table S1.** Luminescent lifetime for complexes, **F1-F8**<sup>a</sup>.

| $\tau$    | N <sub>2</sub> / $\mu$ s | air / ns | O <sub>2</sub> / ns |
|-----------|--------------------------|----------|---------------------|
| <b>F1</b> | 46.96                    | 377.94   | 34.27               |
| <b>F2</b> | 43.86                    | 492.72   | 68.95               |
| <b>F3</b> | 35.09                    | 500.84   | 49.29               |
| <b>F4</b> | 44.30                    | 430.96   | 53.90               |
| <b>F5</b> | 55.42                    | 8.86     | 4.81                |
| <b>F6</b> | 43.48                    | 455.62   | 36.36               |
| <b>F7</b> | 48.15                    | 386.34   | 69.21               |
| <b>F8</b> | 41.16                    | 486.04   | 82.78               |

<sup>a</sup>2.0 × 10<sup>-6</sup> mol L<sup>-1</sup> of the complexes in chloroform at 20 °C.